Cell Stress and Chaperones (2015) 20:121–137
DOI 10.1007/s12192-014-0531-6

ORIGINAL PAPER

A role for the Parkinson's disease protein DJ-1 as a chaperone and antioxidant in the anhydrobiotic nematode *Panagrolaimus superbus*

Bridget A. Culleton · Patrick Lall · Gemma K. Kinsella · Sean Doyle · John McCaffrey · David A. Fitzpatrick · Ann M. Burnell

Received: 16 May 2014 / Revised: 16 July 2014 / Accepted: 28 July 2014 / Published online: 16 October 2014

Abstract Mutations in the human *DJ-1/PARK7* gene are associated with familial Parkinson's disease. DJ-1 belongs to a large, functionally diverse family with homologues in all biological kingdoms. Several activities have been demonstrated for DJ-1: an antioxidant protein, a redox-regulated molecular chaperone and a modulator of multiple cellular signalling pathways. The majority of functional studies have focussed on human DJ-1 (hDJ-1), but studies on DJ-1 homologues in *Drosophila melanogaster*, *Caenorhabditis elegans*, *Dugesia japonica* and *Escherichia coli* also provide evidence of a role for DJ-1 as an antioxidant. Here, we show that dehydration is a potent inducer of a *dj-1* gene in the anhydrobiotic nematode *Panagrolaimus superbus*. Our secondary structure and homology modelling analyses shows that recombinant DJ-1 protein from *P. superbus* (PsuDJ-1.1) is a well-folded protein, which is similar in structure to the hDJ-1. PsuDJ-1.1 is a heat stable protein; with $T_{1/2}$ unfolding transition values of 76 and 70 °C obtained from both circular dichroism (CD) and Fourier transform infrared spectroscopy (FTIR) measurements respectively. We found that PsuDJ-1.1 is an efficient antioxidant that also functions as a 'holdase' molecular chaperone that can maintain its chaperone function in a reducing environment. In addition to its chaperone activity, PsuDJ-1.1 may also be an important non-enzymatic antioxidant, capable of providing protection to *P. superbus* from oxidative damage when the nematodes are in a desiccated, anhydrobiotic state.

Keywords DJ-1 · Chaperone · Antioxidant · Anhydrobiosis · Homology modelling · Molecular dynamics

Abbreviations

BSA	Bovine serum albumin
CD	Circular dichroism
CRYAB	αB-crystallin
CS	Citrate synthase
DTT	Dithiothreitol
EST	Expressed sequence tag
FTIR	Fourier transform infrared spectroscopy
hDJ-1	Human DJ-1
HM	Homology model
MD	Molecular dynamics
MALDI-ToF MS	Matrix-assisted laser desorption/ ionization time of flight mass spectrometry
MWCO	Molecular weight cut-off
Ni-NTA	Nickel nitrilotriacetic acid
PD	Parkinson's disease
PsuDJ-1	*P. superbus* DJ-1
RMSD	Root mean square deviation
ROS	Reactive oxygen species.

Electronic supplementary material The online version of this article (doi:10.1007/s12192-014-0531-6) contains supplementary material, which is available to authorized users.

B. A. Culleton · G. K. Kinsella · S. Doyle · D. A. Fitzpatrick · A. M. Burnell (✉)
Department of Biology, National University of Ireland Maynooth, Maynooth, Co Kildare, Ireland
e-mail: ann.burnell@nuim.ie

P. Lall · J. McCaffrey
Department of Chemistry, National University of Ireland Maynooth, Maynooth, Co Kildare, Ireland

B. A. Culleton
Megazyme International Ireland, Bray Business Park, Bray, Co Wicklow, Ireland

Introduction

Anhydrobiosis is a term used to describe the prolonged, reversible, ametabolic state that some organisms can attain in order to survive conditions of extreme desiccation (Clegg 2001). Anhydrobiotes are capable of losing between 95 and 99 % of their body water during this process (Crowe et al. 1992; Clegg 2001). During anhydrobiosis, metabolism and life processes come to a halt, but they resume again on rehydration. For example, a viable culture of the nematode *Panagrolaimus* sp. PS443 was isolated from dry soil which had been stored in the laboratory for 8 years (Aroian et al. 1993) and embryonated egg cysts of the brine shrimp *Artemia salina* can survive in an anhydrobiotic state for 15 years (Clegg 1967). Some taxa can enter anhydrobiosis at all life stages; these include some bacteria, lichens, mosses, ferns, angiosperm 'resurrection plants', as well as some nematodes, rotifers and tardigrades (Crowe et al. 1992; Clegg 2001; Farrant and Moore 2011). Others have stage-specific forms: spores of some bacteria and fungi, embryonic cysts of brine shrimps and other microcrustaceans, larvae of the chironomid *Polypedilum vanderplanki* and many plant seeds and pollens (Clegg 2001; Alpert 2006; Farrant and Moore 2011).

When cells lose water, the cytoplasm dehydrates and its osmotic strength increases; reactive oxygen species (ROS) accumulate; organelles shrink; membranes change structure from liquid crystalline to gel phase; membrane fusions may occur and many desiccated proteins denature and become prone to aggregation (Crowe et al. 1992; Prestrelski et al. 1993; Clegg 2001; Goyal et al. 2005). Most animals die if they lose more than 15–20 % of their body water (Barrett 1991), while loss of more than 20–50 % of their water content is lethal to most higher plants (Kranner et al. 2002). Anhydrobiotes synthesise a variety of molecules to protect their macromolecules and cellular structures during desiccation (Burnell and Tunnacliffe 2011; Cornette and Kikawada 2011; Farrant and Moore 2011; Hand et al. 2011). These include water replacement molecules such as trehalose or other sugars; antioxidants; molecular chaperones; late embryogenesis abundant (LEA) proteins, which stabilise cellular proteins and prevent their aggregation; and desaturases which adjust membrane fluidity.

An expressed sequence tag (EST) screen of the free-living, anhydrobiotic nematode *Panagrolaimus superbus* identified a homologue of the human *DJ-1* gene which was upregulated in response to desiccation (Tyson et al. 2012). *DJ-1* was first identified as an oncogene that transformed cells in cooperation with activated H-Ras (Nagakubo et al. 1997). Subsequently, it was found that mutations in *DJ-1* were the genetic cause of PARK7 autosomal recessive Parkinson's disease (PD) (Bonifati et al. 2003). Oxidative stress, the aggregation of aberrant and misfolded proteins and dysfunction of the ubiquitin-proteasome system are among the principal molecular events that underlie the pathogenesis of PD (Moore et al. 2005). DJ-1 is ubiquitously expressed in human cells and tissues and is localised in the cytoplasm, mitochondria and nucleus (Canet-Aviles et al. 2004; Kim et al. 2012). Human DJ-1 (hDJ-1) is a member of the large and functionally diverse DJ-1/PfpI family that has homologues distributed across all biological kingdoms (Bandyopadhyay and Cookson 2004; Lucas and Marin 2007). These include *Pyrococcus furiosus* protease I (PfpI) (Halio et al. 1996), the *Escherichia coli* catalase HP-II (Sevinc et al. 1998), the molecular chaperones Hsp31 (Sastry et al. 2002) and YajL (Le et al. 2012) from *E. coli* and isocyanide hydratase from *Pseudomonas fluorescens* (Lakshminarasimhan et al. 2010). Several activities have been demonstrated for hDJ-1—an antioxidant protein (Shendelman et al. 2004; Taira et al. 2004), a molecular chaperone capable of preventing the aggregation of the PD-related protein α-synuclein (Shendelman et al. 2004; Zhou et al. 2006), a modulator of multiple cell signalling pathways (Clements et al. 2006; Waak et al. 2009; Thomas et al. 2011) and an RNA-binding protein (van der Brug et al. 2008). The chaperone activity of hDJ-1 is abolished under reducing conditions suggesting that hDJ-1 is a redox-regulated chaperone that possesses activity only in an oxidising environment (Shendelman et al. 2004).

Human DJ-1 functions as a homodimer in a solution (Wilson et al. 2003). The crystal structures of *E. coli* YajL (Wilson et al. 2005) and *Drosophila melanogaster* DJ-1β (Lin et al. 2012) are strikingly similar to that of hDJ-1—all three molecules form homodimer structures with similar oxidative modification occurring at the nucleophile elbow of the conserved Cys106 residue (Wilson 2011). Thus, a conservation of structure, and possibly function, occurs within the DJ-1 clade. Here, we show that dehydration is a potent inducer of a *dj-1* gene in *P. superbus* and that the recombinant PsuDJ-1.1 protein is an efficient antioxidant that also functions in vitro as a 'holdase' molecular chaperone. The holdase chaperone and antioxidant activity of PsuDJ-1.1, together with the strong and specific transcription of *Psudj-1.1* in response to desiccation, suggests that PsuDJ-1.1 may have an important role in the anhydrobiotic survival of this nematode. Thus, DJ-1 homologues appear to be carrying out analogous protective functions in two different biological processes—desiccation tolerance in an anhydrobiotic nematode and protein homeostasis in human PD neurons.

Materials and methods

Culturing and harvesting *Panagrolaimus superbus*

P. superbus was isolated from a gull's nest in Surtsey (Boström 1988), an icelandic island formed during 1963 to 1967 from volcanic eruptions (Bladursson et al. 2007). It was obtained from Prof. Bjorn Sohlenius, Swedish Museum of Natural History, and is maintained in culture at NUI Maynooth. *P. superbus* was cultured at 20 °C in the dark on nematode growth medium (NGM) plates (Brenner 1974) containing a lawn streptomycin resistant *E. coli* strain HB101 obtained from the *Caenorhabditis* Genetics Center (http://www.cbs.umn.edu/cgc). The NGM was supplemented with streptomycin sulfate (30 μg/mL). Mixed-stage nematodes (i.e. containing a mixture of larvae and adult males and females) were harvested from the NGM plates using distilled water. The nematodes were separated from their *E. coli* food source by sedimentation at room temperature in 50-mL Falcon tubes. The supernatant containing the *E. coli* was removed, and fresh distilled water was added. This washing process was repeated three times.

Cloning the *P. superbus psudj-1.1* gene

RNA was extracted from a mixed population of nematodes using Trizol reagent (Invitrogen), followed by treatment with DNAse I (RNase free, Invitrogen). Total RNA (1 μg per reaction) was converted to complementary DNA (cDNA) using the Transcriptor First Strand cDNA Synthesis Kit (Roche). Using a 200 bp EST sequence (accession number GW413264.1 (Tyson et al. 2012)), the full-length sequence of the *P. superbus dj-1.1* gene was obtained via 5′ and 3′ rapid amplification of cDNA ends (RACE) with a GeneRacer™ kit (Invitrogen). The identity of the amplified sequence was confirmed by DNA sequencing and BLAST analyses at the NCBI database (blast.ncbi.nlm.nih.gov).

Real-time relative qPCR analysis of gene expression

The nematodes were cultured and harvested as described above. The mixed stage nematodes were subjected to stress regimes (selected on the basis of pilot studies), each yielding an 80 % nematode survival rate, compared to a 90 % survival rate for the control worms. Five replicates were prepared for each stress treatment, each replicate containing 3,000 worms in a 1 mL aqueous solution. The stress regimes were as follows: heat stress, 32 °C for 24 h in water; cold stress, 4 °C for 24 h in water; desiccation stress, 98 % relative humidity (RH) for 24 h; osmotic stress, 500 mM sucrose (20 °C for 24 h); oxidative stress, 50 μM methyl viologen in water (20 °C for 24 h). Control nematodes were incubated (in water) at 20 °C for 24 h. For the desiccation treatment, the nematodes were vacuum filtered onto a 2.5 cm Supor 450 filter (Merck Millipore). The filters were then transferred to 3-cm petri dishes without lids and placed in a 10.0-L desiccation chamber containing approximately 300 mL of saturated potassium dichromate ($K_2Cr_2O_7$) which maintained a RH of 98 % (Winston and Bates 1960).

Real-time qPCR reactions were performed using a LightCycler 480 thermocycler and SYBR Green Master I kit (Roche). One microliter of cDNA (prepared as described above) was used for each real-time qPCR reaction. Each reaction also contained 5 μL SYBR Master Mix, 5 pmole of each primer and 2 μL H_20. The primer sequences used were Psudj-1 F: 5′-AGCGCCAGTTATTTTTGCAC-3′ and Psudj-1 R: 5′-CCTGGAGCTCGACTCGTTAC-3′. The PCR cycling conditions used were 40 °C for 10 min, 95 °C 10 min followed by 45 cycles of 95 °C for 10 s, 57 °C for 20 s, 72 °C for 10 s. The *P. superbus ama-1* and *rpl-32* genes were used as internal reference genes, as previously described (Tyson et al. 2012). The expression of *Psudj-1.1* in nematodes exposed to cold, heat, osmotic, desiccation, and oxidative stress relative to *Psudj-1.1* expression in untreated control nematodes was calculated using the $2^{-\Delta\Delta Ct}$ method for relative quantification (Livak and Schmittgen 2001). The Ct value is the number of cycles required for the fluorescent PCR product to reach a specified fluorescence threshold. Melting curve analysis was carried out for each experiment to verify the specificity of the amplification reactions, and we confirmed that the Ct values of the reference genes *ama-1* and *rpl-32* genes were unaffected by the stress treatments. The difference between the Ct values for the *Psudj-1.1* gene and the endogenous control genes is calculated (which gives ΔCt). This provides an internal normalization for each sample. The relative expression (R) of *Psudj-1.1* in the stress-treated versus the control nematodes is $R=2^{-\Delta\Delta Ct}$ where

$$\Delta\Delta Ct = \left[{}^{Ct}_{(Psudj-1.1)} - {}^{Ct}_{(ama-1;rpl-32)}\right]_{\text{treatment}} \div \left[{}^{Ct}_{(Psudj-1.1)} - {}^{Ct}_{(ama-1;rpl-32)}\right]_{\text{control.}}$$

The Ct value used for the endogenous control was the geometric mean of the Ct values obtained for the *ama-1* and *rpl-32* genes. If there is no difference between the treatment and control samples, $2^{-\Delta\Delta Ct}=1$; if $2^{-\Delta\Delta Ct}>1$, *Psudj-1.1* is upregulated in response to the specific stress treatment, and if $2^{-\Delta\Delta Ct}<1$, *Psudj-1.1* is downregulated relative to the untreated control nematodes. An efficiency correction factor (E) is incorporated into the $2^{-\Delta\Delta Ct}$ calculations, thus, $R=(1+E)^{-\Delta\Delta Ct}$. Efficiency estimates were derived from the slope of a standard curve (CT vs log10 dilution factor) generated from a 4-fold serial dilution of pooled cDNAs from all the treatment samples (Pfaffl 2006). Two biological replicates

were assayed for each stress treatment. For each biological replicate, four technical replicates were carried out. Statistically significant differences in expression levels were confirmed using ANOVA, followed by Tukey's post hoc multiple comparisons test ($p<0.05$).

Phylogenetic analyses and sequence comparisons

A representative selection of *dj-1* genes was assembled from BLASTP searches of the NCBI protein database and TBLASTN searches of the EST database (dbEST). EST DNA sequences were translated using Expasy translate tool (http://web.expasy.org/translate/). Only those ESTs encoding full-length sequences were retained. The accession numbers of the sequences used to construct a DJ-1 phylogeny, together with their AA sequences, are presented in Supplementary Table 1. The AA sequences were aligned using MUSCLE (v3.6) (Edgar 2004) with the default settings. Phylogenetic relationships were inferred using maximum likelihood (ML) and Bayesian criteria. For the ML analyses, the appropriate protein model of substitution (WAG+I+G) was selected using ModelGenerator (Keane et al. 2006). One hundred bootstrap replicates were then carried out with the appropriate substitution model using the software program PHYML (Guindon and Gascuel 2003) and summarised using the majority-rule consensus method. The Bayesian phylogeny was reconstructed using PhyloBayes implementing the CAT+G model (Lartillot and Philippe 2008). A posterior consensus tree was obtained by pooling trees from two independent runs, and the analysis was stopped when the observed discrepancy across bipartitions (maxdiff) was less than 0.15. The approximately unbiased test of phylogenetic tree selection (Shimodaira 2002) was performed to assess whether differences in topology between our DJ-1/PfpI protein phylogeny and the accepted metazoan phylogeny (Edgecombe et al. 2011) were no greater than expected by chance.

Homology modelling and model validation

A BLASTp search using the PsDJ-1.1 sequence identified hDJ-1 structures in the Protein Data Bank (PDB, (http://www.rcsb.org/pdb/). PDB: 2R1U, unpublished, had the highest ranked match in the BLASTp search for a hDJ1 that did not contain a mutation and had the highest crystal structure resolution (sequence identity to PsDJ-1.1 34 %, similarity 54 % and coverage 97 %). The 2R1U crystal structure was downloaded from PDB, and Accelrys Discovery Studio Modeling Environment, Release 3.5 (Accelrys Inc., San Diego) was used to prepare the protein structure (add missing atoms, correct connectivity, correct names, etc.). The PsuDJ-1.1 protein sequence was aligned to the hDJ-1 2R1U template, and 1,000 protein structures were built for the alignment using Discovery Studio 3.5. The Modeller software implemented in Discovery Studio 3.5 performs comparative protein structure modelling, by satisfying spatial restraints for C^{α}-C^{α} distances, main-chain N–O distances and main-chain and side-chain dihedral angles (Sali and Blundell 1993; Sali and Overington 1994). Modeller then performs a global optimization procedure to refine the positions of all heavy atoms in the modelled protein. The best model was selected using a combination of the Modeller software Discrete Optimized Protein Energy (DOPE) score and the following protein quality assessment and validation tools: PROCHECK (Laskowski et al. 1996); ERRAT (Colovos and Yeates 1993) and Profiles-3D Verify Score (Bowie et al. 1991). These validation tools were accessed at (http://swift.cmbi.kun.nl/WIWWWI). These are analyses described in greater detail in the Supplementary Material. The final selected model yielded the overall best performance across the validation tools.

Molecular dynamics simulations

Molecular dynamics (MD) simulations were performed using the NAMD 2.10 simulation package (Phillips et al. 2005). The developed PsuDJ-1.1 dimer model was embedded in a solvated box of water molecules (~10,000 water molecules with 15 Å of solvent from the outermost protein perimeter to the box edge). The CHARMM22 force field (MacKerell et al. 1998; Mackerell 2004) was used for proteins, and water molecules were described using TIP3P (Jorgensen et al. 1986). All systems were simulated at 310 K. Temperature and pressure were held constant with Langevin dynamics (Feller, 1995) and the Nosé-Hoover Langevin piston (Nosé, 1984). The particle-mesh Ewald method (Darden, 1993) was used to calculate electrostatic interactions, with a 12 Å cut-off for van der Waals interactions. Briefly, positional harmonic restraints were initially used on the full protein and subsequently on the protein backbone. The restraints were reduced at each subsequent equilibrium simulation. The first two simulations used the NVT (constant volume and temperature) ensemble. A timestep of 1 fs was used for the restrained equilibrium simulations, which were 0.1 ns each. Equilibration without restraints was performed for 1 ns. Production runs (30 ns) began after the systems were equilibrated and used an NPT (constant pressure and temperature) ensemble and a 2 fs timestep. Harmonic restraints were not used in the production runs. Visual Molecular Dynamics 1.9.1 (Humphrey et al. 1996) was used to visualise the simulation trajectories and to perform the root mean square deviation (RMSD) calculations.

Expression and purification of *PsuDJ-1.1*

The *psudj-1.1* gene was inserted into the pET-30LIC expression vector, coding for an N-terminal His_6 tag (Merck

Millipore), and the recombinant plasmid was transformed into *E. coli* BL21 (DE3) pLysS cells (Novagen). Recombinant *E. coli* were grown at 37 °C in LB medium, supplemented with 100 μg/mL kanamycin. Protein expression was induced with the addition of isopropyl-β-D-thiogalactopyranoside to 1 mM followed by incubation at 37 °C for 3 h. Cells were harvested and stored at −80 °C until required. Proteins were extracted using BugBuster protein extraction reagent (Novagen), and all cell lysis extracts were treated with Benzonase nuclease (Novagen). Recombinant PsuDJ-1.1 protein was purified via affinity chromatography on Ni-NTA His bind matrix (Novagen). The protein was further purified by anion exchange chromatography utilizing HiTrap Q HP anion exchange columns attached to an AKTA purifier system (GE Healthcare). The column was washed with five column volumes of start buffer (25 mM Bis-Tris propane, 10 mM NaCl pH 6.5) at a flow rate of 1 mL/min, and the protein sample was applied at a flow rate of 1 mL/min. The column was washed with five column volumes of start buffer until no protein signal was observed. The sample was then eluted using a 0–60 % NaCl gradient over a 20-min period. Purified PsuDJ-1.1 ran as a single band on overloaded sodium dodecyl sulfate polyacrylamide gel electrophoresis (SDS-PAGE) stained with Coomassie blue (Supplementary Fig. 1). The identity of PsuDJ-1.1 was confirmed using Western blotting with a mouse anti-His_6 primary antibody (Roche) and by tryptic in-gel digestion of the purified protein followed by matrix-assisted laser desorption/ionization time of flight (MALDI)-ToF mass spectrometry (Shevchenko et al. 2007). The purified protein was dialysed into storage buffer (20 mM Tris, 10 mM NaCl, 2 mM dithiothreitol (DTT), pH 7.5) and used immediately or stored at −80 °C in aliquots. For each experiment, purified PsuDJ-1.1 was dialysed into the appropriate assay buffer. PsuDJ-1.1 protein concentration was determined spectrophotometrically using a molar extinction coefficient of 7,575 M^{-1} cm^{-1}, calculated using the ProtParam program (http://www.expasy.org/tools/protparam.html). Protein samples were concentrated, when necessary, using Amicon Ultra Centrifugal Filter Devices (Millipore) with a MWCO of 10,000 Da.

Hydrogen peroxide scavenging assay

H_2O_2 concentrations were measured using the scopoletin peroxidase assay (Root 1977; Taira et al. 2004) with minor modifications. Recombinant PsuDJ-1.1 (2.5–10 μM) was incubated with 5 μM H_2O_2 in a final volume of 100 μL for 30 min at 25 °C. At the end of the incubation, 500 μL of 10 mM phosphate-buffered saline (PBS; 137 mM NaCl, 2.7 mM KCl, 10 mM Na_2HPO_4, 1.8 mM KH_2PO_4), 200 μL of 10 mM scopoletin, and 200 μL of 32.5 U/mL horseradish peroxidase were added. After 5 min at 25 °C, the fluorescence of the samples was measured at Ex 366 nm, Em 460 nm using a Cary Eclipse fluorescence spectrometer (Varian) equipped with a Peltier thermostatted cell holder. A standard curve was created in the range 0–20 μM H_2O_2 for the scopoletin peroxidase assay, and the residual H_2O_2 in the experimental samples was calculated from this standard curve. The positive and negative controls were catalase (1 μM) and bovine serum albumin (BSA; 10 μM) respectively. The experiment was repeated three times, and each experiment had three technical replicates. Comparable results were obtained in the replicate experiments. The data presented are from one representative experiment.

Thermal aggregation assay

Citrate synthase (CS) aggregation assays were performed as described by Goyal et al. (Goyal et al. 2005) with minor modifications. Light scattering was measured in a Cary Eclipse fluorescence spectrophotometer (Varian) equipped with a Peltier thermostatted cell holder and a stirred quartz cuvette. Both excitation and emission wavelengths were set to 500 nm. The cuvette containing the assay buffer was pre-incubated at 43 °C for 5 min. CS (from porcine heart, Sigma Aldrich) was then added to a final concentration of 0.30 μM, and the aggregation kinetics were monitored over a 1-h period. Each assay was performed in triplicate. The ability of recombinant PsuDJ-1 to prevent CS aggregation was assayed as follows: PsuDJ-1.1 and CS were suspended in 40 mM N-2-hydroxyethylpiperazine-N-2-ethane sulfonic acid (HEPES)/KOH buffer pH 7.5 at the following molar ratios (CS/PsuDJ-1.1): 3:1, 1:4, 1:10 and 1:20, which correspond, respectively, to 100 nM, 1 μM, 3 μM and 6 μM of PsuDJ-1.1. A positive control, human αB-crystallin (CRYAB), purchased from MyBioSource, was tested at a 1:20 M ratio (CS/CRYAB) corresponding to 6 μM CRYAB. PsuDJ-1.1 and CRYAB were added by substitution of the appropriate volume of reaction buffer in the assay mixture, prior to the addition of CS. The data presented are the mean of three technical replicates from one experiment. Smaller scale experiments were also carried out on five separate occasions and with an independent batch of purified PsuDJ-1.1 to confirm the reproducibility of the aggregation assay between independent batches of PsuDJ-1.1.

Thermal aggregation in a reduced environment

Insulin (10 mg/mL in 25 mM HEPES, pH 8.2) was purchased from Sigma. The assay was carried out in 50 mM Tris/HCl, 2 mM EDTA, pH 8.0. PsuDJ-1.1 was first dialysed into the assay buffer using a PD-10 column (GE Healthcare) according to the manufacturer's instructions. Light scattering was measured in a Cary Eclipse fluorescence spectrophotometer using a Peltier thermostatted cell holder and a stirred quartz cuvette. Both excitation and emission wavelengths were set to 400 nm. For the control experiment, assay buffer and insulin

were added to the cuvette, equilibrated to 25 °C, and insulin aggregation was then initiated by the addition of DTT to a final concentration of 20 mM. The aggregation was monitored for 30 min. The effect of recombinant PsuDJ-1.1 on the DTT-induced aggregation of insulin was studied by including PsuDJ-1.1 in the assay mix to a final concentration of 4 μM, 12 μM or 25 μM. The assay mix was equilibrated to 25 °C, and insulin aggregation was initiated by the addition of DTT as described above. The data presented are the mean of three technical replicates from one experiment. Smaller scale experiments were also carried out on three separate occasions and with an independent batch of purified PsuDJ-1.1 to confirm the reproducibility of the aggregation assay between independent batches of PsuDJ-1.1.

Protease zymography assays

Casein and gelatin zymography was carried out as described by Leber and Balkwill (Leber and Balkwill 1997), with minor modifications. SDS-PAGE gels (12 %) were prepared with the addition of 1 mg/ml casein or gelatin to the resolving gel. Up to 10 μg of PsuDJ-1.1 was loaded on each zymogram, and trypsin (125 ng) was used as a positive control. Following electrophoresis, the SDS was removed from the gel by incubation for 30 min at room temperature with gentle agitation in Tris-Cl pH 7.4 containing 2.5 % Triton X-100. The gel was then rinsed in distilled H_2O, incubated in developing buffer (30 mM Tris-HCl, pH 7.4, 200 mM NaCl, 10 mM $CaCl_2$, and 0.02 % Brij-35 [$C_{12}E_{23}$, polyoxyethylene (23) lauryl ether]) (Sigma-Aldrich) at 30 °C for 12 h and stained with Coomassie brilliant blue (0.5 %). Areas of protease activity appeared as cleared zones against the dark blue background of the stained gel.

Far UV circular dichroism spectroscopy

Far UV circular dichroism (CD) spectra were recorded with a temperature controlled Aviv 400 spectrometer. The final spectrum was taken as a background-corrected average of ten scans carried out under the following conditions: wavelength range, 260–178 nm; temperature, 23 °C; bandwidth, 1 nm; acquisition time, 1 s; intervals, 0.2 nm. Measurements were performed in a 0.01 cm cell using 1.0 mg/mL PsuDJ-1.1 in 10 mM potassium phosphate, 100 mM potassium fluoride buffer pH 7.0. To observe the effect of oxidation on PsuDJ-1.1, the sample was oxidised with H_2O_2 to final concentrations of 50–500 mM. The effect of a reduced environment on the secondary structure of PsuDJ-1.1 was studied by adding DTT to a final concentration of 5 mM to the assay mix. Quantitative secondary structure analysis was performed using the SELCON3, CONTIN/LL, CDSSTR, VARSLC and K2D algorithms on the DICHROWEB server (Whitmore and Wallace 2004). CD_{222} melt experiments were performed for PsuDJ-1.1 using a 1 cm quartz cell (Hellma, UK) equipped with a magnetic stirrer, at a wavelength of 222 nm, a spectral acquisition time of 1 s, over a temperature range of 10–88 °C, stepped at 3 °C, with an equilibration time for each step of 2 min. The $T_{½}$ value for native PsuDJ-1.1 was determined as the temperature at which the CD_{222} intensity had decreased by half of its total intensity over the temperature range of the experiment.

FTIR spectroscopy

Fourier transform infrared spectroscopy (FTIR) spectra were acquired for native PsuDJ-1.1 using a Tensor 27 FTIR spectrometer (Bruker Optik, Gmbh), equipped with a sensitive liquid N_2 cooled MCT detector (Bruker Optik, Gmbh). The assays were performed in 10 mM PBS, pH 7.5 (137 mM NaCl, 2.7 mM KCl, 10 mM Na_2HPO_4, 1.8 mM KH_2PO_4), and the PsuDJ-1.1 protein concentration was 5 mg/mL. Transmission spectra were acquired using an AquaSpec transmission cell accessory (Bruker Optik, Gmbh). Norton-Beer Fourier-transformed background-corrected absorption spectra were taken at 20 °C between 1,000 and 4,000 cm^{-1} as an average of 150 scans, acquired at a resolution of 4 cm^{-1} and an optical aperture of 0.5 cm. All spectra were post-processed using OPUS software (Bruker Optik). An atmospheric correction algorithm was utilised to remove any water vapour bands from final absorption spectra. Spectra were zeroed between 1,750 and 1,800 cm^{-1}, and the 2nd derivative spectra were calculated.

Results and discussion

Dehydration is a potent inducer of the *psudj-1.1* gene in the anhydrobiotic nematode *P. superbus*

A *P. superbus* gene with homology to the DJ-1/PfpI family which was identified in an EST screen was shown to be upregulated in response to desiccation (Tyson et al. 2012). We used 5′ and 3′ RACE to obtain the coding sequence of this gene, designated *Psudj-1.1* (GenBank accession number KJ522972). The sequence contained a 558 bp open reading frame. *Psudj-1.1* was strongly transcribed in response to desiccation stress (Fig. 1), where its relative expression levels increased 12-fold ($p<0.05$, Tukey's post hoc multiple comparisons test). Slight but statistically insignificant increases in transcription levels occurred in response to osmotic stress (2.2-fold), cold (1.8-fold), oxidative stress (1.5 fold) and heat (1.1-fold). DJ-1 is widely associated with the response to oxidative stress (Taira et al. 2004; Lin et al. 2012; Tsushima et al. 2012), so its minimal response to oxidative stress in *P. superbus* is surprising. Instead, the potent induction of

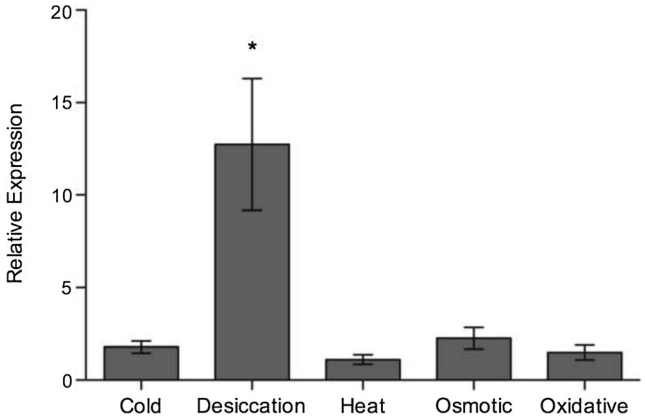

Fig. 1 Real-time relative qPCR analysis of the expression of the *Panagrolaimus superbus dj-1.1* gene in response to cold, heat, osmotic, desiccation and oxidative stress. The reference genes were the *P. superbus rpl-32* and *ama-1* genes (Tyson et al. 2012). Data are the mean of eight measurements (two biological replicates, each containing four technical replicates). Statistically significant differences ($p<0.05$, Tukey's post hoc multiple comparisons test) are indicated, *$p<0.05$

Psudj-1.1 in response to desiccation suggests that a major function of DJ-1.1 in *P. superbus* may be in anhydrobiotic protection. Accumulation of *dj-1* transcripts has also been associated with desiccation stress in other systems. A screen for desiccation-responsive genes in the anhydrobiotic nematode *Aphelenchus avenae* found that *dj-1* transcripts were upregulated in response to desiccation and hyperosmotic conditions (Reardon et al. 2010). RNA-seq transcription profiles of of diapausing, desiccation-resistant embryos of the rotifer *Brachionus plicatilis* also show enrichment for *dj-1* transcripts (Clark et al. 2012). Stress-resistant dauer larvae of *Caenorhabditis elegans* accumulate abundant *dj-1* transcripts in response to desiccation stress, as shown in a recent microarray analysis, where this gene was among the top ten most highly upregulated desiccation-response genes (Erkut et al. 2013). Erkut et al. also showed that *C. elgans* dauer larvae in which *dj-1* function was eliminated by deletion mutation had their capacity to survive exposure to 60 % RH reduced from 91.1 % in the controls to 79.9 % in the mutant nematodes ($p>0.05$).

Phylogenetic analyses and sequence comparisons

A pairwise comparison of the percentage of AA residues in alignments of DJ-1/PfpI sequences which are shared between taxa shows that there is a very strong conservation of AA identity among vertebrate DJ-1 sequences, whereas much greater sequence variability occurs among members of the invertebrate phyla, including the Nematoda (Supplementary Table 2). For example, the pairwise AA identity between *P. superbus* DJ-1.1 and *C. elegans* DJ1.1 is 48 % and that between *P. superbus* DJ-1.1 and *Brugia malyai* DJ1 is 39 %, whereas the DJ-1 sequences of human and mouse are 92 % identical, and human and zebrafish (*Danio rerio*) sequences share 83 % sequence identity. A duplication of the *dj-1* gene has occurred in *D. melanogaster* and in the *Caenorhabditis* clade. The extent of *dj-1* gene duplication in other invertebrate taxa is difficult to determine at present due to incomplete genome sequence and/or assembly data. However, our database searches did not reveal evidence of widespread duplication of the *dj-1* gene in invertebrates.

A ML phylogeny of DJ-1/PfpI sequences from eukaryote and bacterial phyla (Fig. 2) shows that, despite the greater degree of sequence variability within the invertebrate phyla, a within-phylum relatedness of DJ-1 sequences is evident. However, the phylogenetic signal in these DJ-1 sequences is not sufficient to return the well-established evolutionary relationships between the invertebrate phyla (Edgecombe et al. 2011). For example, the flatworm species *Dugesia japonica* and *Schmidtea mediterranea* are grouped with the Nematoda; the Nematoda and Arthropoda are not returned as sister clades and the Chordata and Echinodermata (Deuterostomia) are not returned as a sister clade to the other invertebrate phyla (Protosomia). A Bayesian tree also returned a similar topology to the ML phylogeny (data not presented). The approximately unbiased test of phylogenetic tree selection (Shimodaira 2002) shows that placing the Plathyhelminthes as the sister group to the Annelida and Mollusca (Edgecombe et al. 2011) is significantly worse than the phylogeny obtained using DJ-1 sequences. Similarly, a constrained tree that places the Chordata and Echinodermata as the sister clade to other invertebrate phyla (Protosomia) is also significantly worse than our DJ-1 protein phylogeny. However, the relationships between and within Bacteria and Fungi and between the Chordate taxa in our DJ-1/PfpI phylogeny do correspond to the established evolutionary relationships. Overall, these observations suggest that the DJ-1 proteins may have lineage specific rates of evolution, particularly within invertebrate phyla, and are consequently are not ideal phylogenetic markers.

Multiple sequence alignment and homology modelling of PsuDJ-1.1

Alignment of the amino acid (AA) sequence of PsuDJ-1.1 with key orthologs (Fig. 3) shows that, despite a sequence identity of only 33 % between PsuDJ-1.1 and hDJ-1 in this multiple sequence alignment (Supplementary Table 2), the secondary structure of PsuDJ-1.1 appears to be strongly conserved. The hDJ-1 monomer comprises 11 β-sheets and 8 α-helices (Huai et al. 2003; Lee et al. 2003; Tao and Tong 2003; Wilson et al. 2003). Human DJ-1, *E. coli* YajL and *D. melanogaster* DJ-1β all function as obligate dimers, and crystal studies show that the DJ-1 dimers from human, *Drosophila* DJ-1β and YajL have an extensive interface between the two monomers (Wilson et al. 2003, 2005; Lin et al.

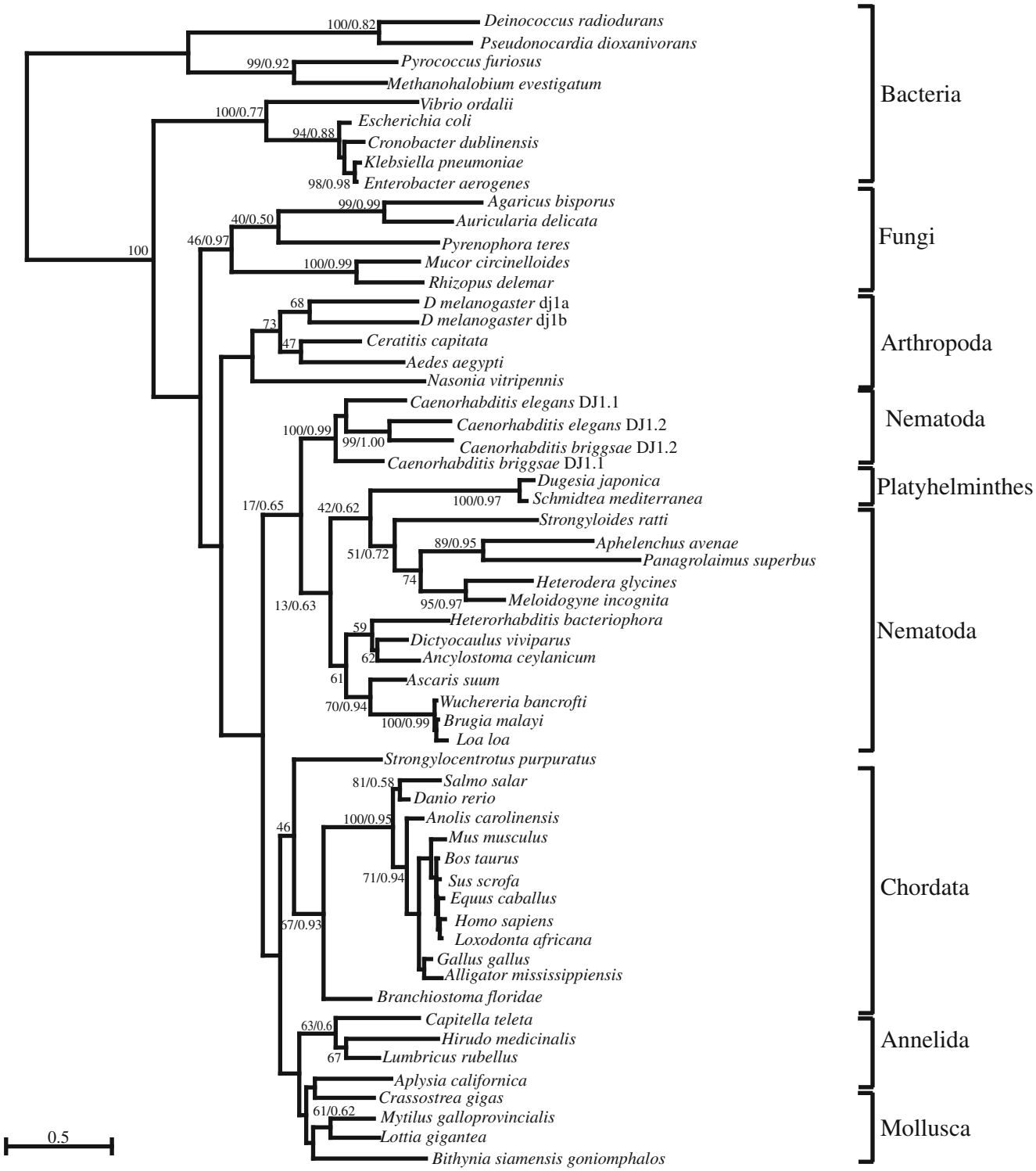

Fig. 2 Hypothesis of phylogenetic relationships of DJ-1/PfpI family protein sequences from bacterial and eukaryote phyla inferred using the maximum likelihood criterion. These sequences, together with their accession numbers, are presented in Supplementary Table 1. Maximum likelihood bootstrap supports are shown for all branches and Bayesian probabilities for selected branches

2012). Residues at the dimer interface of hDJ-1 (Tao and Tong 2003) are indicated in Fig. 3, as well as functionally important sites that have been implicated in PD pathogenesis.

Using the crystal structure of hDJ-1, an homology model of PsuDJ-1.1 was developed (Fig. 4; Supplementary Fig. 2) and structurally validated (Supplementary Table 3). Both the hDJ-

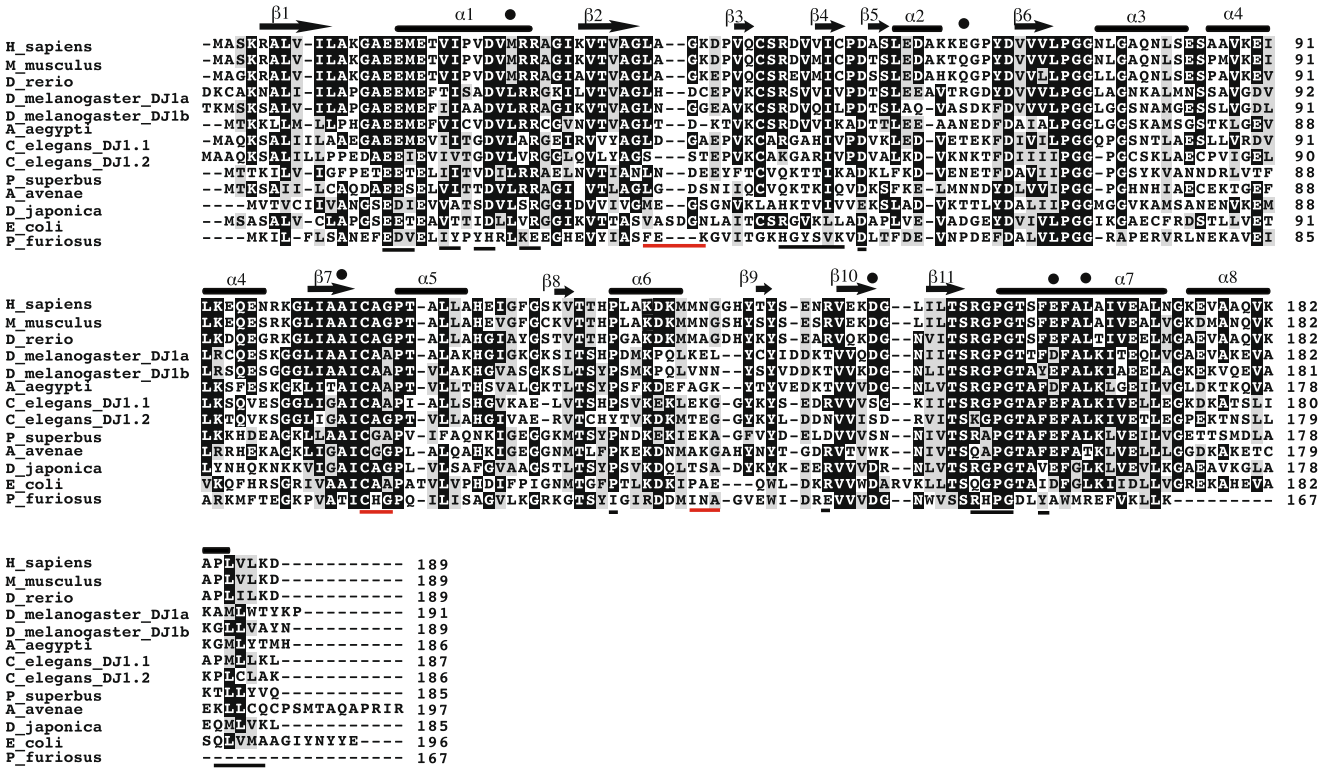

Fig. 3 Alignment of the amino acid sequence of *Panagrolaimus superbus* DJ-1.1 with key orthologous sequences. The aligned DJ-1/PfpI sequences are as follows: *Homo sapiens* (NP009193.2), *Mus musculus* (NP065594.2), *Danio rerio* (NP001005938.1), *Drosophila melanogaster* DJ-1alpha (NP610916.1) and DJ1-beta (NP651825.3), *Aedes aegypti* (XP001648396.1), *Caenorhabditis elegans* DJ-1.1 (NP493696.1) and DJ-1.2 (NP504132.1), *Panagrolaimus superbus* (KJ522972), *Aphelenchus avenae* (GR463903.1), *Dugesia japonica* (BAM68888.1), *Escherichia coli* YajL (Q46948.2) and *Pyrococcus furiosus* PfpI protease (NP_579448.1). We have used the amino acid numbering of *Homo sapiens* DJ-1.1. Where more than 50 % of the amino acids in a column are identical, these identical amino acids are indicated by a *black background*; a *grey background* indicates amino acids which are similar to the column consensus (in charge, *shape* and size) and a *white background* indicates unrelated amino acids. The structural annotations for *H. sapiens* DJ-1.1 are taken from the hDJ-1 crystal structure (PDB: 2R1U, Supplementary Table 4) and from UniProt (http://www.uniprot.org/uniprot/Q99497). The residues in the dimer interface are *underlined in black* (data from Tao and Tong 2003). Turns are indicated by *red lines*. Residues implicated in PD pathogenesis (M26, E64, A104, D149, E163, L166) are indicated by *filled black circles*—details and references are provided in the text

1 template (PDB/2R1U) and the initial PsuDJ-1.1 homology model contained 11 β strands and 8 α-helices (Supplementary Table 4). To examine whether the 3D conformation of the homology model was stable, it was subjected to 30 ns aqueous solvent MD simulation. The RMSD of a representative MD-simulated structure from that of the initial PsuDJ-1.1 homology model was low at 1.776 Å, indicating a stable protein conformation in this fold (Supplementary Fig. 2a). When the refined MD model of the PsuDJ1-1 dimer was overlaid on the hDJ1 template structure (Supplementary Fig. 2b), an RMSD of 1.834 Å was achieved—an indication of the strong conservation of 3D conformation between the two structures.

The residues in the active site involved in H_2O_2 scavenging in hDJ-1 are Glu18, Gly75, Ala107 and Cys106 (Wilson 2011), and these are highly conserved in invertebrate sequences, as well as in *E. coli* YajL (Fig. 3). AAs at three of six sites implicated in familial PD (Malgieri and Eliezer 2008) are conserved in PsuDJ-1.1: Ala104, Glu163, Leu166; while three Met26, Glu64 and Asp149 are not conserved in the nematode protein. Met26 is conserved in vertebrates but is replaced by Leu in other clades; Glu64 is not conserved in vertebrates or in invertebrates, being frequently replaced in vertebrates by Gln and in invertebrates by a variety of uncharged residues—Asn, Gln, Ser, Thr; D149 is strongly conserved in the DJ-1 family, with the exception of the Nematoda where it is replaced by a diversity of aliphatic amino acids, predominantly Ser and Thr. A Cys46Ala substitution has been shown to reduce the stability of hDJ-1 (Canet-Aviles et al. 2004), and Cys46 is conserved in PsuDJ-1.1. The locations of these residues discussed above are indicated in PsuDJ-1.1 homology model (Fig. 4a).

Helices α-1, α-7 and α-8, along with the β-3, β-4 and β-11 sheets are involved in dimer formation in hDJ-1 (Tao and Tong 2003). The canonical Leu166Pro human PARK7 mutation (Bonifati et al. 2003) introduces a Pro residue into α-7 that disrupts the hydrophobic interactions between α-helices 7 and 8, destabilising the dimer interface (Honbou et al. 2003; Huai et al. 2003; Lee et al.

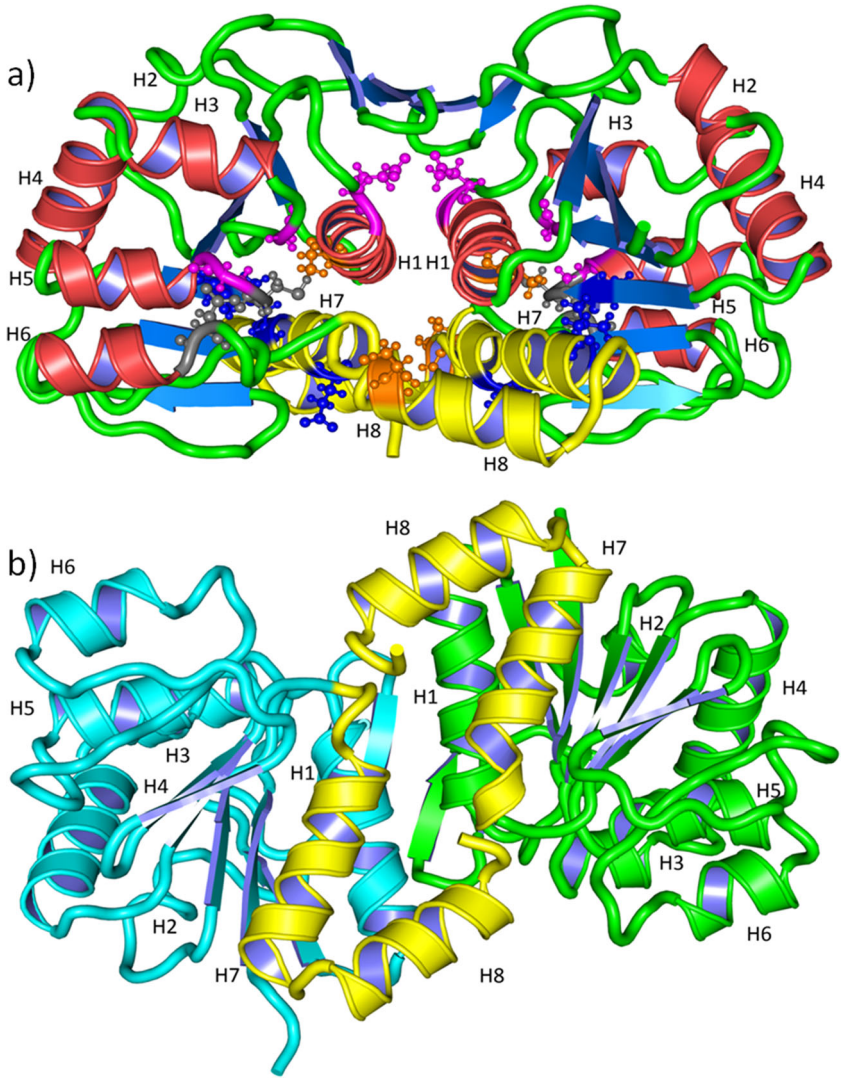

Fig. 4 **a**, **b** Representative snapshots of the generated homology model of the PsuDJ-1.1 dimer after 30 ns of molecular dynamics simulation. In **a** the nucleophile elbow of the conserved Cys106 and the PsuDJ-1.1 His126Tyr substitution are in *grey*; the sites involved in H_2O_2 scavenging are in *magenta*; familial PD sites are in *blue*; the Pro22Thr and Pro184Thr sites are in *orange*. The hydrophobic patch formed by α-helices 7 and 8 is in *yellow*. The view in **b** is rotated by 90° with respect to the view in **a** to visualise the hydrophobic patch (*yellow*). The remainder of monomers in **b** are illustrated in *green* and *cyan* respectively. Image generated using Pymol (DeLano 2002)

2003; Tao and Tong 2003; Wilson et al. 2003). Because of its unique geometry and its non-reactive side chain, proline has a strong propensity to destabilise α-helices in proteins (Pace and Scholtz 1998; Betts 2003). Interestingly, two Pro residues that are present in vertebrate DJ-1 sequences (Pro22 and Pro184) are not generally conserved in other taxa. In PsuDJ-1.1, a Pro22Thr substitution occurs in the α-1 helix involved in dimer formation, and a Pro184Thr substitution occurs in the α-8 helix, which is also involved in dimer formation. These substitutions may lead to a more stable dimer molecule in the nematode.

A hydrophobic patch formed by the C-terminal α-helices 7 and 8 is the proposed site of hDJ-1 molecular chaperone activity (Lee et al. 2003), and deletion of residues 174–189 results in a significant reduction in the chaperone activity of hDJ-1 (Lee et al. 2003). Twelve of 16 residues in the hDJ-1 α-7 helix are strictly conserved between hDJ-1 and PsuDJ-1.1. For the α-8 helix, only one residue is conserved between the two sequences; however, 8 of the 11 residues in α-8 are hydrophobic in PsuDJ-1.1, suggesting that α-helices 7 and 8 also form a hydrophobic patch in the nematode protein. The coaxial arrangement of these two C-terminal α-helices, (α-7 and -8), in the hydrophobic patch at the surface of the dimer interface in the PsuDJ-1.1 model is highlighted in Fig. 4b.

Production of recombinant PsuDJ-1.1

Recombinant PsuDJ-1.1 was purified to homogeneity using affinity and anion exchange chromatography, and it corresponded to one species at approximately 24 kDa on a 12 % SDS-PAGE gel (Supplementary Fig. 1). The identity of the recombinant PsuDJ-1.1 protein was confirmed using mass spectrometry (Supplementary Table 5). The recombinant pET-30LIC expression vector containing the *PsuDJ-1.1* gene insert has been deposited in the Addgene repository (www.addgene.org; deposit number 52080).

The secondary structure content of *PsuDJ-1.1*

The secondary structure of PsuDJ-1.1 was investigated using CD (Fig. 5a) and FTIR spectroscopy (Fig. 5b, c). The CD spectrum of PsuDJ-1.1 shows the presence of a characteristic α-helical band with minima at 222 and 208 nm (Fig. 5a). The presence of significant β-sheet content is evident from the shift in the characteristic positive α-helical band at 193 to 195 nm. Oxidation of PsuDJ-1.1 with up to 600 mM H_2O_2 revealed no loss of secondary structure, as determined by its CD spectrum. Similarly, no change in secondary structure was observed upon reduction of PsuDJ-1.1 with 5 mM DTT (Fig. 5a). Analysis of the 2nd derivative amide-1 FTIR spectrum (Fig. 5c) reveals two intense bands centred at 1,653 and 1,628 cm^{-1}. The 1,653 cm^{-1} band results from the presence of α-helix content while that at 1,628 cm^{-1} indicates β-sheets. Minor β-sheet and turn bands are also present at 1,687 and 1,674 cm^{-1} respectively. These data show that PsuDJ-1.1 is a well-folded protein that has helical and sheet conformations in approximate proportion to that of the crystal structure of hDJ-1.

PsuDJ-1.1 is an effective scavenger of hydrogen peroxide

The accumulation of ROS is triggered by cellular dehydration (Pereira et al. 2003; Kranner and Birtic 2005; Franca et al. 2007). Hence, anhydrobiotes require mechanisms to detoxify ROS, maintain redox homeostasis and repair ROS-mediated damage to macromolecules. Human DJ-1 and its homologues in *Drosophila* and *Dugesia* have a role in preventing the accumulation of H_2O_2 in vivo (Andres-Mateos et al. 2007; Stefanatos et al. 2012; Tsushima et al. 2012), and hDJ-1 is a potent scavenger of H_2O_2 in vitro (Taira et al. 2004; Andres-Mateos et al. 2007). PsuDJ-1.1 effectively eliminates H_2O_2 in a concentration-dependent manner in vitro (Fig. 6). At a 1:1 M equivalent ratio, PsuDJ-1.1 eliminated H_2O_2 within a 5-min incubation period. Strong antioxidant activity was also observed for catalase, a positive control, while bovine serum albumin, which is known to interact with hydrogen peroxide through its single Cys residue (Davies et al. 1993), had statistically insignificant antioxidant effect. Removal of the N-terminal His_6 tag with enterokinase showed no effect on activity (data not shown).

Many enzymatic antioxidant defense systems are upregulated in response to desiccation or osmotic stress in microorganisms, plants and animals (Franca et al. 2007; Rizzo et al. 2010; Burnell and Tunnacliffe 2011). Enzymatic antioxidants require aqueous conditions. Thus, they can provide protection against ROS activity only during the induction and recovery phases of anhydrobiosis. The PsuDJ-1.1 molecule contains two oxidizable cysteines and three oxidizable methionines, and it functions as an efficient scavenger of H_2O_2 in vitro. PsuDJ-1.1 may therefore be an important non-enzymatic antioxidant capable of providing protection from ROS damage to the nematodes when they are in a dry anhydrobiotic state.

PsuDJ-1.1 acts as molecular chaperone that can function in a reducing environment

Human DJ-1 has been shown to function as a molecular chaperone in vitro where it prevents the heat-induced aggregation of CS (Lee et al. 2003; Shendelman et al. 2004), luciferase (Lee et al. 2003) and glutathione S-transferase (Shendelman et al. 2004), and it also prevents the formation of protofibrils of the PD-related protein α-synuclein (Shendelman et al. 2004). The *E. coli* DJ-1 homologue YajL was also found to have chaperone activity, using denatured CS and the ribosomal proteins S1 and L3 as substrates (Kthiri et al. 2010). Similarly, we have found that PsuDJ-1.1 can prevent the heat-induced aggregation of CS in a concentration-dependent manner in the absence of ATP (Fig. 7). Suppression of CS aggregation was evident at a 1:0.3 M ratio (CS/PsuDJ-1.1) and at a 1:20 M ratio (CS/PsuDJ-1.1), PsuDJ-1.1 completely suppressed the aggregation of 0.3 μM CS over a 1-h incubation period. Removal of the N-terminal His_6 tag with enterokinase showed no effect on activity (data not shown). The positive control, the holdase chaperone αB-crystallin (Kulig and Ecroyd 2012), also showed molecular chaperone activity towards CS at a 1:20 M ratio, although its activity was less than that seen for PsuDJ-1.1. When proteins denature, their exposed hydrophobic regions interact with hydrophobic regions from adjacent unfolding proteins, forming insoluble cytotoxic aggregates (Kiefhaber et al. 1991; Sharma et al. 2009). Holdase chaperones such as αB-crystallin and other small heat shock proteins (sHsp) maintain aggregation-prone substrates in an unfolded yet soluble state by passively binding to, and sequestering, exposed hydrophobic surfaces (Sharma et al. 2009). These holdases maintain unfolded proteins in a refolding-competent state, until cellular conditions are permissive for ATP-dependent chaperones (such as Hsp70) to restore them back to their native conformation (Kulig and Ecroyd 2012).

Shendelman *et al.* (2004) found that hDJ-1 failed to suppress the aggregation of reduced insulin and that pre-incubation of hDJ-1 with DTT abolished hDJ-1 chaperone activity in the CS aggregation assay. The highest molar ratio (insulin/hDJ-1) tested by Shendelman *et al.* (2004) in these assays was 1:0.15. These authors proposed that DJ-1 functions as a redox-sensitive molecular chaperone that possesses chaperone activity only in an oxidizing environment. The mechanism by which cysteine oxidation alters human DJ-1 function is unclear because the crystal structures of reduced and Cys106-sulfinate-oxidised hDJ-1 proteins are 'essentially identical' (Lin et al. 2012). We find that incubation of PsuDJ-1.1 with insulin in the presence of DTT results in a

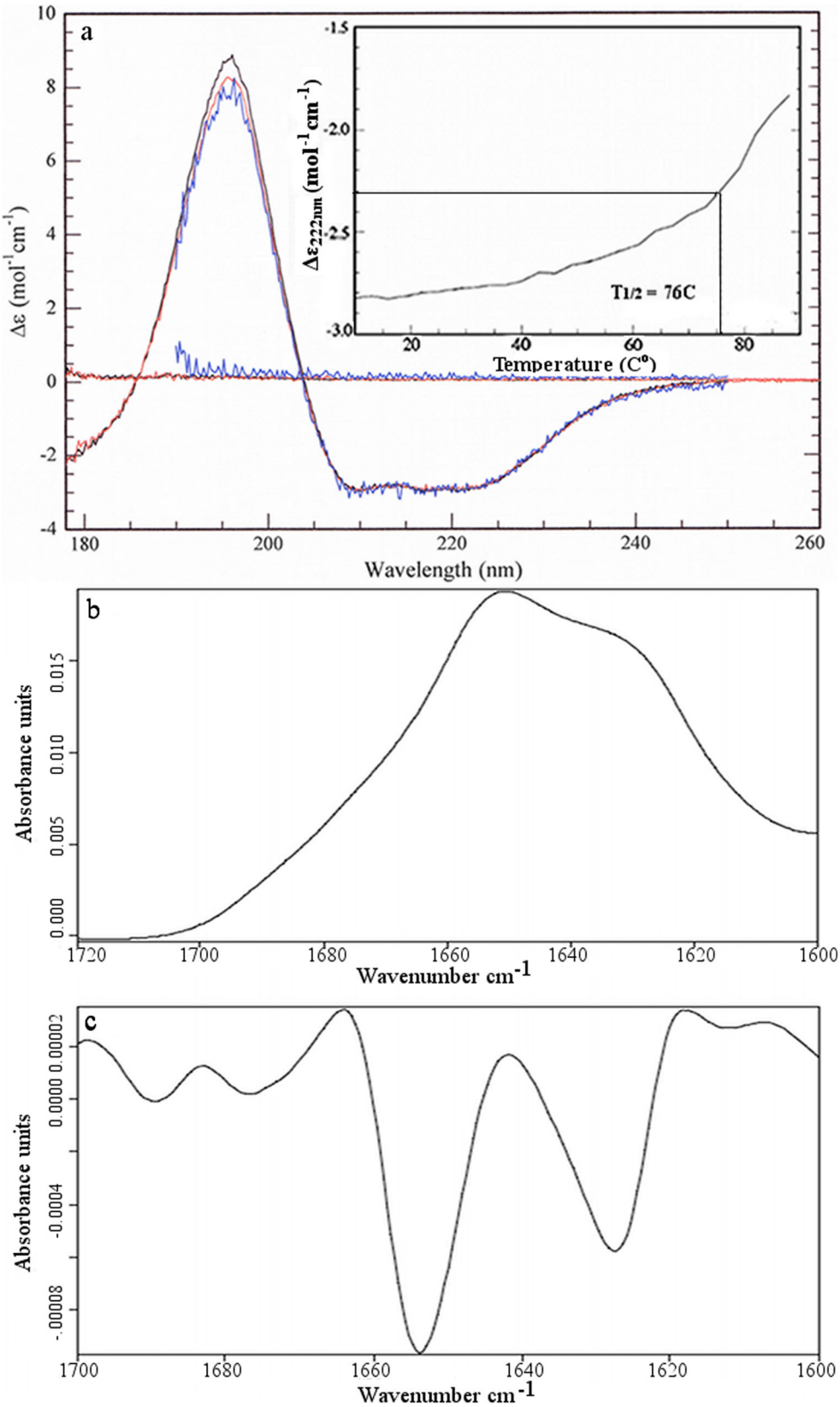

Fig. 5 The secondary structural content of of native PsuDJ-1.1 as revealed by CD and FTIR spectroscopy at 23 °C. **a** CD spectrum of native, native, oxidized and reduced PsuDJ-1.1 at pH 7.0. *Black line*, native PsuDJ-1.1; *red line*, oxidized PsuDJ-1.1 (treated 600 mM H_2O_2), *blue line*, reduced PsuDJ-1.1 (treated with 5 mM DTT). The line at approximately zero on the y-*axis* indicates deviations from average amplitude. *Inset*: CD spectral analysis of the heat stability of native PsuDJ-1.1. The increase in absorbance of the α-helix (Δε) at 222 nm was monitored as a function of temperature; **b** Gaussian *curve* fitted to the amide I FTIR absorption spectrum; **c** the second derivative of the amide I absorption spectrum

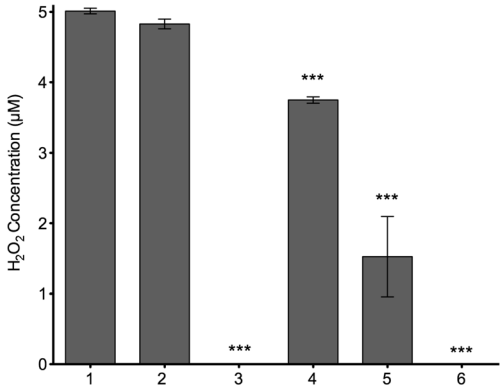

Fig. 6 The elimination of hydrogen peroxide by PsuDJ-1.1. Recombinant PsuDJ-1 (2.5 –10 μM) was incubated with 5 μM H_2O_2 in a final volume of 100 μL for 30 min at 25 °C. At the end of the incubation period, the residual H_2O_2 in the experimental samples was measured using a scopoletin peroxidase assay (Root 1977; Taira et al. 2004). Catalase (1 μM) and bovine serum albumin (BSA) 10 (μM) were used as controls. 1, H_2O_2 (5 μM) alone; 2, BSA (10 μM)+H_2O_2; 3, catalase (1 μM)+H_2O_2; 4, PsuDJ-1 1.25 μM+H_2O_2; 5, PsuDJ-1 2.5 μM+H_2O_2; 6, PsuDJ-1 5 μM+H_2O_2. The experiment was repeated three times. Comparable results were obtained in each experiment. Data are the mean±SD, n=3 from one representative experiment. Statistically significant differences are indicated (data were analysed using one-way ANOVA followed by with Dunnett's post hoc test for multiple comparisons), ***p<0.001

concentration-dependent chaperone activity (Fig. 8). Suppression of insulin aggregation was evident at a 1:0.26 M ratio (insulin/PsuDJ-1.1), and at a 1:0.55 M ratio (insulin/PsuDJ-1.1), PsuDJ-1.1 decreased the aggregation of insulin by 49.5 % following incubation for 30 min in a reducing environment. These results indicate that nematode DJ-1.1 would be functional in a reducing environment, which normally exists in cytoplasm (Go and Jones 2008) and not just when oxidising conditions occur.

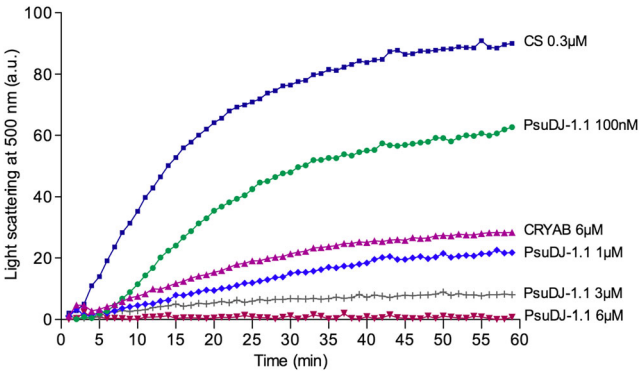

Fig. 7 The ability of PsuDJ-1.1 to prevent the thermal aggregation of citrate synthase (CS) at 43 °C. The aggregation of CS (0.3 μM) was monitored at excitation and emission wavelengths of 500 nm following the addition of CS plus 100 nM PsuDJ-1.1 (1:0.3), *green circle*; or CS plus 1 μM PsuDJ-1.1 (1:3.3) *violet diamond*; or CS plus 3 μM PsuDJ-1.1 (1:10), *cross*; or CS+6 μM PsuDJ-1.1 (1:20), *inverted triangle*; or CS plus 6 μM αB-crystallin (1:20), *pink triangle*; or CS alone, *blue square*; [molar ratios (CS: PsuDJ-1.1) in brackets]. Data are the mean, n=3 from one representative experiment

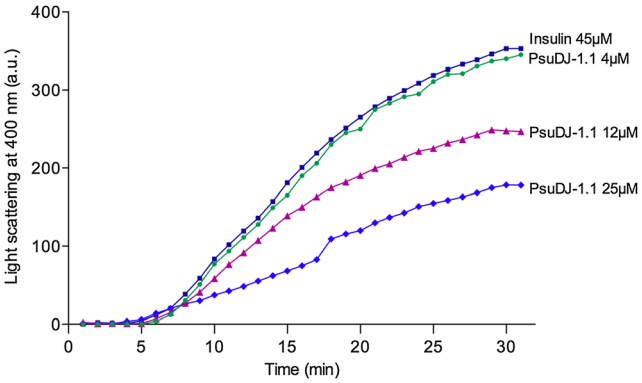

Fig. 8 The ability of PsuDJ-1.1 to suppress the DTT induced aggregation of insulin at 25 °C. The aggregation of the insulin B-chain (45 μM) in the presence of 20 mM DTT was measured at 400 nm. Insulin alone, *blue square*; insulin plus 4 μM PsuDJ-1.1 (1:0.09), *green circle*; insulin plus 12 μM PsuDJ-1.1 (1:0.26), *pink triangle*; insulin plus 25 μM PsuDJ-1.1 (1:0.55), *violet diamond*; [molar ratios (insulin: PsuDJ-1.1) in brackets]. Data are the mean, n=3 from one representative experiment

The ability to detect, stabilise, repair or remove damaged proteins is essential for the anhydrobiotic organism. In addition to classical molecular chaperones, anhydrobiotes also utilise chemical chaperones such as trehalose (Crowe et al. 1992) and sucrose (Farrant and Moore 2011), as well as novel protein chaperones such as artemin (Warner et al. 2004; Chen et al. 2007) and natively unfolded hydrophilic LEA proteins (Goyal et al. 2005), to prevent protein aggregation during desiccation. *Psudj-1.1* is strongly upregulated in response to desiccation stress and shows only minimal responses to the other stresses tested, including oxidative stress. The potent holdase activity of PsuDJ-1.1, together with the strong and specific transcription of *Psudj-1.1* in response to desiccation, suggests that PsuDJ-1.1 plays a role in the anhydrobiotic protection of this nematode.

Native PsuDJ-1.1 lacks protease activities in vitro

Some prokaryotic members of the DJ-1/PfpI family possess potent protease activity (Du et al. 2000; Quigley et al. 2003). These proteases have a Cys-His-Glu/Asp catalytic triad, which is absent in proteins from the DJ-1 clade. We found no evidence of protease activity for native PsuDJ-1.1 using zymography, with either gelatin or casein as substrate (Supplementary Fig. 4). Removal of the N-terminal His_6 tag with enterokinase led to identical results (data not shown). Cleavage of the 15-amino acid C-terminus sequence of hDJ-1 confers a cysteine protease capability, with a catalytic efficiency (kcat/Km) which is 65-fold less than that of trypsin (Chen et al. 2010). These authors propose that hDJ-1 protease activation most probably results from the formation of a catalytic dyad between Cys106 and His126. The His126 residue is conserved among vertebrate DJ-1 homologues (Bandyopadhyay and Cookson 2004), and in some

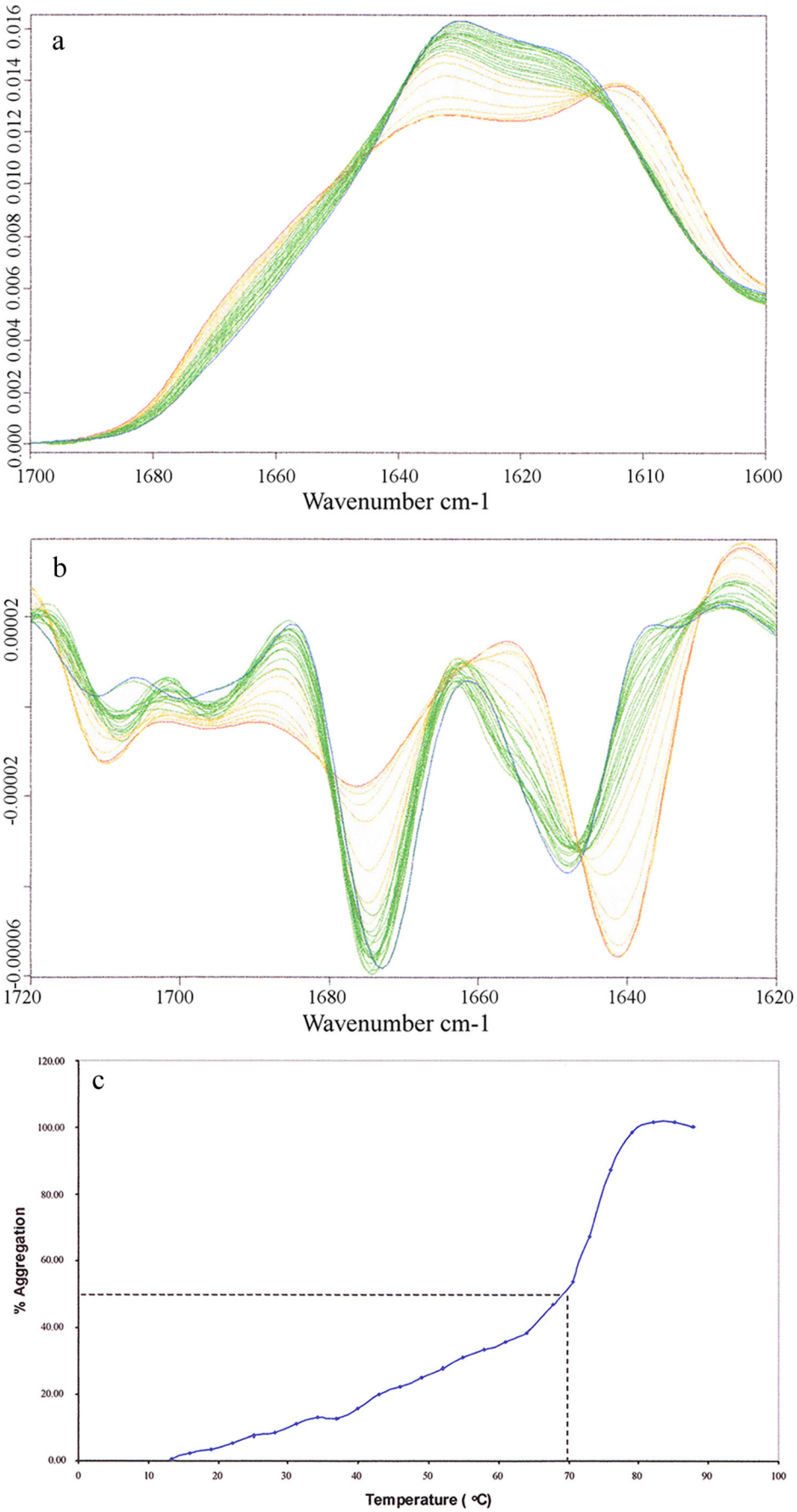

Fig. 9 FTIR spectral analysis of the heat stability of PsuDJ-1.1. **a** Gaussian *curve* fitted to the FTIR absorption spectrum of the amide I band of PsuDJ-1.1. The colours show the transition of the temperature gradient as follows: *blue* 13 °C, *green* 16–61 °C, *orange* 64–85 °C, *red* 88 °C, **b** the second derivatives of the amide I spectra show an increase in the characteristic protein aggregation band at ~1,622 cm^{-1} of the PsuDJ-1.1 protein, **c** the aggregation profile of PsuDJ-1.1, monitored by the increase in intensity of the 1,622 cm^{-1} band as a function of temperature

invertebrates, including *C. elegans*. However, in PsuDJ-1.1 and *D. melanogaster* DJ-1β, this His126 residue is replaced by Tyr (Fig. 3), which would prevent a hydrogen-bonding interaction with the catalytic cysteine residue (Lin et al. 2012). This provides structural evidence that PsuDJ-1.1 is unlikely to function as a protease, although further studies with PsuDJ-1.1 lacking the C-terminal region would be necessary to confirm this.

PsuDJ-1.1 is thermostable

High thermal stability values are characteristic of molecular chaperones (Sastry et al. 2002; Warner et al. 2004; Kwon et al. 2008). We examined the thermal stability of the helix domains of native PsuDJ-1.1 using CD spectral analysis by monitoring the change in ellipticity ($\Delta\varepsilon$) of the helix domains at 222 nm as a function of temperature. A $T_{1/2}$ unfolding transition of 76 °C was observed for PsuDJ-1.1 (Fig. 5a), which agrees well with the $T_{1/2}$ unfolding transition of 77 °C at 222 nm for native hDJ-1 (Malgieri and Eliezer 2008). The global thermal stability of the helix domains of PsuDJ-1.1 was also investigated using FTIR spectroscopy (Fig. 9a, b), where the amide-I spectral region was monitored for the presence of a characteristic 'protein aggregation band' occurring at 1,622 cm^{-1} over an increasing temperature gradient between (13–88 °C). PsuDJ-1.1 thermostability determined by FTIR measurements had a $T_{1/2}$ value of 70 °C (Fig. 9c). These results show that PsuDJ-1.1 is heat stable, with transition midpoint values of 76 °C and 70 °C being found using CD and FTIR techniques respectively. The discrepancy between the CD and FTIR $T_{1/2}$ values is consistent with helices being the most stable component of protein secondary structures.

Conclusions

DJ-1 is a multifunctional protein that may play an important role in anhydrobiotic protection in the nematode *P. superbus*. The *Psudj-1.1* gene is strongly transcribed in response to desiccation stress but shows statistically non-significant transcription responses to osmotic, oxidative, heat and cold stresses. In in vitro assays, recombinant PsuDJ-1.1 protein is an efficient antioxidant and also functions as a holdase molecular chaperone, being more effective at inhibiting the thermal aggregation of CS than an equimolar concentration of the well-characterised chaperone αB-crystallin (Reddy et al. 2006). Unlike hDJ-1, PsuDJ-1.1 maintains its chaperone function in a reducing environment. Our secondary structure and homology modelling analyses shows that PsuDJ-1.1 is a well-folded protein, which is similar in structure to the hDJ-1. PsuDJ-1.1 is a heat stable protein, with $T_{1/2}$ unfolding transition values of 76 °C and 70 °C obtained, respectively, from CD and FTIR measurements. AA sequence comparisons show that PsuDJ-1.1 and several other invertebrate taxa differ from hDJ-1 in having two P→T substitutions in α-1 and α-9, which are located in the putative dimer interface of PsuDJ-1.1. These substitutions may give rise to more compact α-helices, which could confer dimer stability to the nematode protein. PsuDJ-1.1 contains two oxidizable cysteines and three oxidizable methionines, and it functions as an efficient scavenger of H_2O_2 in vitro. Thus, in addition to its holdase chaperone activity, PsuDJ-1 may also be an important non-enzymatic antioxidant, capable of providing protection to *P. superbus* from ROS damage when the nematodes are in a desiccated, anhydrobiotic state. Because of its importance as the genetic cause of PARK7 familial PD, studies on DJ-1 to date have focussed on the protective functions of DJ-1 in vertebrate and invertebrate neurons. Our data show that some members of the DJ-1 family may have a more general role as an antioxidant and protein chaperone in dehydrated cells and tissues.

Acknowledgments This project was funded by Science Foundation Ireland (Projects 08/RFP/EOB1660 and 09/RFP/EOB2506). BAC was funded by an Irish Research Council EMBARK post-graduate fellowship. qPCR facilities were funded by Science Foundation Ireland (SFI/07/RFP/GEN/F571/EC07). The AKTA Purifier and MALDI-ToF MS were funded by the Irish Higher Education Authority and the Irish Health Research Board, respectively. The authors wish to acknowledge the DJEI/DES/SFI/HEA Irish Centre for High-End Computing (ICHEC) for the provision of computational facilities and support. The NAMD 2.10 simulation package was developed with NIH support by the Theoretical and Computational Biophysics Group in the Beckman Institute for Advanced Science and Technology at the University of Illinois at Urbana-Champaign.

References

Alpert P (2006) Constraints of tolerance: why are desiccation-tolerant organisms so small or rare? J Exp Biol 209:1575–1584

Andres-Mateos E et al (2007) DJ-1 gene deletion reveals that DJ-1 is an atypical peroxiredoxin-like peroxidase. Proc Natl Acad Sci U S A 104:14807–14812

Aroian R, Carta L, Kaloshian I, Sternberg P (1993) A free-living *Panagrolaimus* sp. from Armenia can survive anhydrobiosis for 8.7 years. J Nematol 25:500–502

Bandyopadhyay S, Cookson MR (2004) Evolutionary and functional relationships within the DJ1 superfamily. BMC Evol Biol 4:9

Barrett J (1991) Anhydrobiotic nematodes. In: Evans K (ed) Agricultural zoology reviews Intercept Ltd. Andover, England, pp 161–176

Betts MJ, Russell RR (2003) Amino acid properties and consequeces of substitutions. In: Barnes MR, Gray, I.C. (ed) Bioinformatics for Geneticists, John Wiley and Sons, pp 289–316

Bladursson S, Ingadóttir Á (eds) (2007) Nomination of Surtsey for the UNESCO world heritage list. Icelandic Institute of Natural History, Reykjavík

Bonifati V et al (2003) Mutations in the DJ-1 gene associated with autosomal recessive early-onset parkinsonism. Science 299:256–259

Boström S (1988) Descriptions and morphological variability of three populations of *Panagrolaimus* Fuchs, 1930 (Nematoda, Panagrolaimidae). Nematologica 34:144–155

Bowie JU, Lüthy R, Eisenberg D (1991) A method to identify protein sequences that fold into a known three-dimensional structure. Science 253:164–170

Brenner S (1974) The genetics of *Caenorhabditis elegans*. Genetics 77: 71–94

Burnell AM, Tunnacliffe A (2011) Gene induction and desiccation stress in nematodes. In: Perry RN, Wharton DA (eds) Molecular and physiological basis of nematode survival. CAB International, Wallingford, Oxfordshire, pp 125–156

Canet-Aviles RM et al (2004) The Parkinson's disease protein DJ-1 is neuroprotective due to cysteine-sulfinic acid-driven mitochondrial localization. Proc Natl Acad Sci U S A 101:9103–9108

Chen T, Villeneuve TS, Garant KA, Amons R, MacRae TH (2007) Functional characterization of artemin, a ferritin homolog synthesized in *Artemia* embryos during encystment and diapause. FEBS J 274:1093–1101

Chen J, Li L, Chin L-S (2010) Parkinson disease protein DJ-1 converts from a zymogen to a protease by carboxyl-terminal cleavage. Hum Mol Genet 19:2395–2408

Clark MS et al (2012) Long-term survival of hydrated resting eggs from *Brachionus plicatilis*. PLoS One 7:e29365

Clegg JS (1967) Metabolic studies of cryptobiosis in encysted embryos of *Artemia salina*. Comp Biochem Physiol 20(20):801–809

Clegg JS (2001) Cryptobiosis—a peculiar state of biological organization. Comp Biochem Physiol B Biochem Mol Biol 128:613–624

Clements CM, McNally RS, Conti BJ, Mak TW, Ting JP (2006) DJ-1, a cancer- and Parkinson's disease-associated protein, stabilizes the antioxidant transcriptional master regulator Nrf2. Proc Natl Acad Sci U S A 103:15091–15096

Colovos C, Yeates T (1993) Verification of protein structures: patterns of nonbonded atomic interactions. Protein Sci 2:1511–1519

Cornette R, Kikawada T (2011) The induction of anhydrobiosis in the sleeping chironomid: current status of our knowledge. IUBMB Life 63:419–429

Crowe JH, Hoekstra FA, Crowe LM (1992) Anhydrobiosis. Annu Rev Physiol 54:579–599

Darden T, York D, Pedersen L (1993) Particle mesh Ewald: An N log(N) method for Ewald sums in large systems. J Chem Phys 98:10089–10092

Davies MJ, Gilbert BC, Haywood RM (1993) Radical-induced damage to bovine serum albumin: role of the cysteine residue. Free Radic Res Commun 18:353–367

Darden T, York D and Pedersen L (1993) Particle mesh Ewald: An Nlog(N) method for Ewald sums in large systems. J Chem Phys 98:10089–10092

DeLano WL (2002) The PyMOL Molecular Graphics System. In. DeLano Scientific LLC, San Carlos, CA, USA. http://www.pymol.org

Du XL et al (2000) Crystal structure of an intracellular protease from *Pyrococcus horikoshii* at 2-angstrom resolution. Proc Natl Acad Sci U S A 97:14079–14084

Edgar RC (2004) MUSCLE: multiple sequence alignment with high accuracy and high throughput. Nucl Acids Res 32:1792–1797

Edgecombe GD et al (2011) Higher-level metazoan relationships: recent progress and remaining questions. Org Divers Evol 11:151–172

Erkut C, Vasilj A, Boland S, Habermann B, Shevchenko A, Kurzchalia TV (2013) Molecular strategies of the *Caenorhabditis elegans* dauer larva to survive extreme desiccation. PLoS One 8:e82473

Farrant JM, Moore JP (2011) Programming desiccation-tolerance: from plants to seeds to resurrection plants. Curr Opin Plant Biol 14:340–345

Franca MB, Panek AD, Eleutherio ECA (2007) Oxidative stress and its effects during dehydration. Comp Biochem Physiol A Mol Integr Physiol 146:621–631

Feller S. E, Zhang Y. H, Pastor R. W, Brooks B. R (1995) Constant pressure molecular dynamics simulation: The Langevin piston method. J Chem Phys 103:4613–4621

Go Y-M, Jones DP (2008) Redox compartmentalization in eukaryotic cells. Biochim Biophy Acta 1780:1273–1290

Goyal K, Walton LJ, Tunnacliffe A (2005) LEA proteins prevent protein aggregation due to water stress. Biochem J 388:151–157

Guindon S, Gascuel O (2003) A simple, fast, and accurate algorithm to estimate large phylogenies by maximum likelihood. Syst Biol 52: 696–704

Halio S, Blumentals I, Short S, Merrill B, Kelly R (1996) Sequence, expression in *Escherichia coli*, and analysis of the gene encoding a novel intracellular protease (PfpI) from the hyperthermophilic archaeon *Pyrococcus furiosus*. J Bacteriol 178:2605–2612

Hand SC, Menze MA, Toner M, Boswell L, Moore D (2011) LEA proteins during water stress: not just for plants anymore. Annu Rev Physiol 73:115–134

Honbou K et al (2003) The crystal structure of DJ-1, a protein related to male fertility and Parkinson's disease. J Biol Chem 278:31380–31384

Huai Q et al (2003) Crystal structure of DJ-1/RS and implication on familial Parkinson's disease. FEBS Lett 549:171–175

Humphrey W, Dalke A, Schulten K (1996) VMD: visual molecular dynamics. J Mol Graph 14(33–38):27–38

Jorgensen WL, Chandrasekhar J, Buckner JK, Madura JD (1986) Computer simulations of organic reactions in solution. Ann N Y Acad Sci 482:198–209

Keane TM, Creevey CJ, Pentony MM, Naughton TJ, McLnerney JO (2006) Assessment of methods for amino acid matrix selection and their use on empirical data shows that ad hoc assumptions for choice of matrix are not justified. BMC Evol Biol 6:29

Kiefhaber T, Rudolph R, Kohler HH, Buchner J (1991) Protein aggregation in vitro and in vivo—a quantitative model of the kinetic competition between folding and aggregation. Nat Biotechnol 9:825–829

Kim S-J, Park Y-J, Hwang I-Y, Youdim MBH, Park K-S, Oh YJ (2012) Nuclear translocation of DJ-1 during oxidative stress-induced neuronal cell death. Free Radic Biol Med 53:936–950

Kranner I, Birtic S (2005) A modulating role for antioxidants in desiccation tolerance. Integr Comp Biol 45:734–740

Kranner I, Beckett RP, Wornik S, Zorn M, Pfeifhofer HW (2002) Revival of a resurrection plant correlates with its antioxidant status. Plant J 31:13–24

Kthiri F et al (2010) Protein aggregation in a mutant deficient in YajL, the bacterial homolog of the parkinsonism-associated protein DJ-1. J Biol Chem 285:10328–10336

Kulig M, Ecroyd H (2012) The small heat-shock protein alpha B-crystallin uses different mechanisms of chaperone action to prevent the amorphous versus fibrillar aggregation of alpha-lactalbumin. Biochem J 448:343–352

Kwon S, Jung Y, Lim D (2008) Proteomic analysis of heat-stable proteins in *Escherichia coli*. BMB Rep 41:108–111

Lakshminarasimhan M, Madzelan P, Nan R, Milkovic NM, Wilson MA (2010) Evolution of new enzymatic function by structural modulation of cysteine reactivity in *Pseudomonas fluorescens* isocyanide hydratase. J Biol Chem 285:29651–29661

Lartillot N, Philippe H (2008) Improvement of molecular phylogenetic inference and the phylogeny of Bilateria. Phil Trans R Soc B 363: 1463–1472

Laskowski R, Rullmannn J, MacArthur M, Kaptein R, Thornton J (1996) AQUA and PROCHECK-NMR: programs for checking the quality of protein structures solved by NMR. J Biomol NMR 8:477–486

Le H-T et al (2012) YajL, prokaryotic homolog of parkinsonism-associated protein DJ-1, functions as a covalent chaperone for thiol proteome. J Biol Chem 287:5861–5870

Leber TM, Balkwill FR (1997) Zymography: a single-step staining method for quantitation of proteolytic activity on substrate gels. Anal Biochem 249:24–28

Lee SJ et al (2003) Crystal structures of human DJ-1 and *Escherichia coli* Hsp31, which share an evolutionarily conserved domain. J Biol Chem 278:44552–44559

Lin J, Prahlad J, Wilson MA (2012) Conservation of oxidative protein stabilization in an insect homologue of parkinsonism-associated protein DJ-1. Biochemistry 51:3799–3807

Livak KJ, Schmittgen TD (2001) Analysis of relative gene expression data using real-time quantitative PCR and the 2-[Delta] [Delta] CT method. Methods 25:402–408

Lucas JI, Marin I (2007) A new evolutionary paradigm for the Parkinson disease gene DJ-1. Mol Biol Evol 24:551–561

Mackerell AD (2004) Empirical force fields for biological macromolecules: overview and issues. J Comput Chem 25:1584–1604

MacKerell AD et al (1998) All-atom empirical potential for molecular modeling and dynamics studies of proteins. J Phys Chem B 102: 3586–3616

Malgieri G, Eliezer D (2008) Structural effects of Parkinson's disease linked DJ-1 mutations. Protein Sci 17:855–868

Moore DJ, West AB, Dawson VL, Dawson TM (2005) Molecular pathophysiology of Parkinson's disease. Annu Rev Neurosci 28:57–87

Nagakubo D et al (1997) DJ-1, a novel oncogene which transforms mouse NIH3T3 cells in cooperation with ras. Biochem Biophys Res Commun 231:509–513

Nosé S. A, (1984) unified formulation of the constant temperature molecular-dynamics methods. J Chem Phys 81:511–519

Pace CN, Scholtz JM (1998) A helix propensity scale based on experimental studies of peptides and proteins. Biophys J 75:422–427

Pereira EJ, Panek AD, Eleutherio ECA (2003) Protection against oxidation during dehydration of yeast. Cell Stress Chaperon 8:120–124

Pfaffl MW (2006) Relative quantification. In: Dorak T (ed) Real-time PCR. Taylor and Francis Group, New York, pp 63–82

Phillips JC et al (2005) Scalable molecular dynamics with NAMD. J Comput Chem 26:1781–1802

Prestrelski SJ, Tedeschi N, Arakawa T, Carpenter JF (1993) Dehydration-induced conformational transitions in proteins and their inhibition by stabilizers. Biophys J 65:661–671

Quigley PM, Korotkov K, Baneyx F, Hol WGJ (2003) The 1.6-angstrom crystal structure of the class of chaperones represented by *Escherichia coli* Hsp31 reveals a putative catalytic triad. Proc Natl Acad Sci U S A 100:3137–3142

Reardon W et al (2010) Expression profiling and cross-species RNA interference (RNAi) of desiccation-induced transcripts in the anhydrobiotic nematode *Aphelenchus avenae*. BMC Mol Biol 11:6

Reddy GB, Kumar PA, Kumar MS (2006) Chaperone-like activity and hydrophobicity of alpha-crystallin. IUBMB Life 58:632–641

Rizzo AM et al (2010) Antioxidant defences in hydrated and desiccated states of the tardigrade *Paramacrobiotus richtersi*. Comp Biochem Physiol B Biochem Mol Biol 156:115–121

Root RK (1977) H_2O_2 release from human granulocytes during phagocytosis. J Clin Invest 60:1266–1279

Sali A, Blundell T (1993) Comparative protein modelling by satisfaction of spatial restraints. J Mol Biol 234:779–815

Sali A, Overington J (1994) Derivation of rules for comparative protein modeling from a database of protein structure alignments. Protein Sci 3:1582–1596

Sastry MSR, Korotkov K, Brodsky Y, Baneyx F (2002) Hsp31, the *Escherichia coli yedU* gene product, is a molecular chaperone whose activity is inhibited by ATP at high temperatures. J Biol Chem 277:46026–46034

Sevinc M, Switala J, Bravo J, Fita I, Loewen P (1998) Truncation and heme pocket mutations reduce production of functional catalase HPII in *Escherichia coli*. Protein Eng 11:549–555

Sharma SK, Christen P, Goloubinoff P (2009) Disaggregating chaperones: an unfolding story. Curr Protein Pept Sci 10:432–446

Shendelman S, Jonason A, Martinat C, Leete T, Abeliovich A (2004) DJ-1 is a redox-dependent molecular chaperone that inhibits alpha-synuclein aggregate formation. PLoS Biol 2:1764–1773

Shevchenko A, Tomas H, Havlis J, Olsen JV, Mann M (2007) In-gel digestion for mass spectrometric characterization of proteins and proteomes. Nat Protoc 1:2856–2860

Shimodaira H (2002) An approximately unbiased test of phylogenetic tree selection. Syst Biol 51:492–508

Stefanatos R et al (2012) dj-1β regulates oxidative stress, insulin-like signaling and development in *Drosophila melanogaster*. Cell Cycle 11:3876–3886

Taira T, Saito Y, Niki T, Iguchi-Ariga SMM, Takahashi K, Ariga H (2004) DJ-1 has a role in antioxidative stress to prevent cell death. EMBO Rep 5:213–218

Tao X, Tong L (2003) Crystal structure of human DJ-1, a protein associated with early onset Parkinson's disease. J Biol Chem 278: 31372–31379

Thomas KJ et al (2011) DJ-1 acts in parallel to the PINK1/parkin pathway to control mitochondrial function and autophagy. Hum Mol Genet 20:40–50

Tsushima J et al (2012) Protective effect of planarian DJ-1 against 6-hydroxydopamine-induced neurotoxicity. Neurosci Res 74:277–283

Tyson T et al (2012) A molecular analysis of desiccation tolerance mechanisms in the anhydrobiotic nematode *Panagrolaimus superbus* using expressed sequenced tags. BMC Res Notes 5:68

van der Brug MP et al (2008) RNA binding activity of the recessive parkinsonism protein DJ-1 supports involvement in multiple cellular pathways. Proc Natl Acad Sci U S A 105:10244–10249

Waak J et al (2009) Oxidizable residues mediating protein stability and cytoprotective interaction of DJ-1 with apoptosis signal-regulating kinase 1. J Biol Chem 284:14245–14257

Warner AH, Brunet RT, MacRae TH, Clegg JS (2004) Artemin is an RNA-binding protein with high thermal stability and potential RNA chaperone activity. Arch Biochem Biophys 424:189–200

Whitmore L, Wallace BA (2004) DICHROWEB, an online server for protein secondary structure analyses from circular dichroism spectroscopic data. Nucl Acids Res 32:W668–673

Wilson MA (2011) The role of cysteine oxidation in DJ-1 function and dysfunction. Antioxid Redox Signal 15:111–122

Wilson MA, Collins JL, Hod Y, Ringe D, Petsko GA (2003) The 1.1-angstrom resolution crystal structure of DJ-1, the protein mutated in autosomal recessive early onset Parkinson's disease. Proc Natl Acad Sci U S A 100:9256–9261

Wilson MA, Ringe D, Petsko GA (2005) The atomic resolution crystal structure of the YajL (ThiJ) protein from *Escherichia coli*: a close prokaryotic homologue of the Parkinsonism-associated protein DJ-1. J Mol Biol 353:678–691

Winston PW, Bates PS (1960) Saturated salt solutions for the control of humidity in biological research. Ecology 41:232–237

Zhou WB, Zhu M, Wilson MA, Petsko GA, Fink AL (2006) The oxidation state of DJ-1 regulates its chaperone activity toward α-synuclein. J Mol Biol 356:1036–1048